Nanoscale

PAPER

View Article Online
View Journal | View Issue

Cite this: *Nanoscale*, 2025, **17**, 8170

Selenium nanoparticles: influence of reducing agents on particle stability and antibacterial activity at biogenic concentrations†

Aneta Bužková,[a] Lucie Hochvaldová,[a] Renata Večeřová,[b] Tomáš Malina,[c] Martin Petr,[c] Josef Kašlík,[c] Libor Kvítek,[a] Milan Kolář,[b] Aleš Panáček*[a] and Robert Prucek*[a]

Selenium nanoparticles (SeNPs) have recently attracted attention for their antimicrobial and anticancer activities. Nevertheless, their use remains limited due to stability issues. The objective of this study is to investigate the impact of different reaction conditions (including the reducing and stabilizing agents, as well as reaction temperature) on the water dispersion characteristics, stability, and biological activity of SeNPs. The particle characteristics were controlled using sodium borohydride as a strong reducing agent and ascorbic acid as a mild agent. The impact of different stabilizers, namely sodium oleate, quercetin, gelatine, poly(ethyleneimine), and poly(diallyldimethyl-ammonium chloride), was investigated on both particle stability and biological activity. Several destabilizing processes occurred, one of which was continuous reduction to the final Se(-II) oxidation state, which was observed in both synthetic approaches, with using sodium borohydride or ascorbic acid as reducing agents. Non-stabilized SeNP dispersions were stable for a maximum of two weeks, while most stabilized SeNP dispersions remained stable for at least two months, and some remained stable for as long as six months. The antibacterial activity had strong effects, particularly against Gram-positive bacteria, and simultaneously low cytotoxicity against mammalian cells. SeNPs exhibited significant antibacterial efficacy, particularly against *Staphylococcus aureus*, including methicillin-resistant *Staphylococcus aureus* strains, even at concentrations as low as 1 mg L^{-1}. SeNPs synthesized utilizing sodium borohydride demonstrate minimal cytotoxicity (EC_{50} > 100 mg L^{-1}). Interestingly, SeNPs reduced by ascorbic acid demonstrated higher cytotoxicity (EC_{50} 6.8 mg L^{-1}) against the NIH/3T3 cell line. This effect is likely due to the combined cytotoxic effect of SeNPs and ascorbic acid acting as a pro-oxidant at high concentrations.

Received 13th December 2024,
Accepted 16th February 2025

DOI: 10.1039/d4nr05271d

rsc.li/nanoscale

1. Introduction

Since the discovery of antibiotics, several bacteria, including methicillin-resistant *Staphylococcus aureus* (MRSA) and vancomycin-resistant *Enterococcus species* (VRE), have developed resistance to these drugs, resulting in severe complications in the treatment of infections caused by them.[1–4] The issue of bacterial resistance affects not only human medicine but also veterinary medicine, and may result in significant economic losses in the future.[3] Consequently, novel antibacterial agents are continually being developed, including analogues of existing compounds and newly synthesized molecules. Over the past 15 years, an emerging group of nanostructured antibacterial materials, called 'nanoantibiotics', has also been intensively developed and studied. As the field of nanotechnology continues to expand, numerous nanomaterials have been investigated for their antimicrobial properties.[4–8] Silver nanoparticles represent a typical example of nanoantibiotics, exhibiting considerable potential in antibacterial treatments and applications due to their extraordinary antibacterial properties.[9] However, silver is a heavy metal element[10] that can be distributed within a wide range of organs, potentially causing genotoxicity and hepatic, renal, neurological, and hematologi-

[a]*Department of Physical Chemistry, Faculty of Science, Palacký University, 17. listopadu 1192/12, 779 00 Olomouc, Czech Republic. E-mail: robert.prucek@upol.cz, ales.panacek@upol.cz*
[b]*Department of Microbiology, Faculty of Medicine and Dentistry, Palacký University, Hněvotínská 3, 779 00 Olomouc, Czech Republic*
[c]*Regional Centre of Advanced Technologies and Materials (RCPTM), Czech Advanced Technology and Research Institute (CATRIN), Palacký University, Šlechtitelů 241/27, 779 00 Olomouc, Czech Republic*

†Electronic supplementary information (ESI) available: As mentioned in the text, additional figures include the remaining TEM images, changes in the UV-vis absorption spectra of all discussed dispersions, and a zoom on the first 30 days of size and zeta potential changes in the discussed selenium nanoparticle dispersions. See DOI: https://doi.org/10.1039/d4nr05271d

cal toxicity at certain concentrations.[11] Selenium, on the other hand, is an allotropic metalloid[12] and is an essential micronutrient for several major metabolic pathways.[13] Unfortunately, despite its essentiality, this element is toxic to all organisms in high doses. Due to its both harmful and beneficial properties, it is called an 'essential poison'.[14] It has been reported that inorganic forms of selenium are more toxic than its nanoforms,[15] likely due to the lower solubility of nanoparticles compared to that of inorganic compounds.[16] As a result, selenium nanoparticles (SeNPs) have gained interest due to their low toxicity and enhanced anticancer and antimicrobial activities.[12]

SeNPs can be synthesized using several techniques. Chemical methods are the most commonly used, as they are highly reliable and easy to use.[17] The most common approaches for synthesizing SeNPs from soluble salt precursors employ reducing methods utilizing glutathione,[18,19] ascorbic acid[6,20–23] or sodium borohydride.[5] Additionally, biological methods using microorganisms[24,25] or plant extracts[26,27] have become increasingly popular in recent years. Spherical zero-dimensional (0D) nanostructures of SeNPs are mainly formed *via* chemical or biological approaches.[17] In contrast, physical techniques can be used for the preparation of nanostructures such as nanobelts, nanowires,[28] microtubes,[29] hollow microspheres, microflowers, microrods,[30] and nanofibers.[31] Spherical SeNPs typically exhibit strong biological properties, while anisotropic nanostructures demonstrate strong electrochemical, catalytic, or photoconductive properties.[17] Unfortunately, despite their intriguing properties, SeNPs show high instability,[12] which results in the rapid loss of their attractive properties. However, the stability of nanoparticles can be improved through surface modification using various surfactants and polymers during particle synthesis, thus preserving the unique properties of the SeNPs, including antibacterial activity.[32] The antibacterial activity of SeNPs has been reported in numerous studies, with demonstrated biological efficacy and minimum inhibitory concentrations (MICs) varying significantly over a wide range, from 2 to 250 mg L^{-1}. The reported differences in the MIC values of SeNPs can be attributed to the dependence of the antibacterial efficacy on the synthesis method of SeNPs,[5] the stabilizing agent used,[21] and the type of bacterial strain tested.[6] It is therefore evident that the antibacterial activity of SeNPs, in addition to the particle characteristics, is also significant and mainly influenced by their aggregation stability. Unlike silver nanoparticles, their activity is also influenced by the type of bacteria tested, which can be either Gram-positive or Gram-negative, differing in their cell wall structure.

In this study, different synthetic conditions were investigated, including the use of sodium borohydride and ascorbic acid as strong and mild reducing agents, respectively. Furthermore, the synthesis of SeNPs with different particle characteristics was investigated, with the objective of developing a highly stable dispersion that exhibits high antibacterial activity and low cytotoxicity towards mammalian cells. This was achieved by varying the reaction temperature and using different surface stabilizers.

2. Materials and methods

2.1. Materials

Sodium selenite, sodium borohydride, quercetin, sodium oleate and poly(diallyldimethyl-ammonium chloride) (PDDA, 20% water solution; 200 000–350 000 M_W) were purchased from Sigma-Aldrich Chemical Co. Hydrochloric acid (32% water solution) and gelatine were obtained from Lach-Ner. L-Ascorbic acid was obtained from Penta. Poly(ethyleneimine) (PEI, 600 000 Da, 50% water solution) was purchased from Honeywell Fluka. All materials were obtained in their purest form available, designated as p.a. quality.

For the antibacterial assay, Mueller–Hinton agar was purchased from Bio-Rad. The Gram-negative bacterial strains *Escherichia coli* CCM 3954 and *Pseudomonas aeruginosa* CCM 3955, and the Gram-positive strains *Enterococcus faecalis* CCM 4224 and *Staphylococcus aureus* CCM 4223 were obtained from the Czech Collection of Microorganisms (Masaryk University, Brno). Vancomycin-resistant *Enterococcus faecium* (VRE) 419 and methicillin-resistant *Staphylococcus aureus* (MRSA) 4591 strains were obtained from the culture collection of the Department of Microbiology (Faculty of Medicine and Dentistry, Palacký University Olomouc).

For cytotoxicity testing, the tetrazolium dye for the MTT assay was purchased from Sigma Aldrich. The NIH/3T3 cells were obtained from the American Type Culture Collection (ATCC, USA), while Dulbecco's modified Eagle's medium (DMEM) was sourced from Life Technologies.

2.2. Synthesis and stabilization of SeNPs

The synthesis of selenium nanoparticle (SeNP) dispersions was achieved through the chemical reduction method, utilizing either sodium borohydride or ascorbic acid as a reducing agent. Non-stabilized SeNPs were prepared at a temperature of 25 or 90 °C. When sodium borohydride was used, a 50 mL dispersion of non-stabilized SeNPs was prepared as follows. 5 mL of 0.01 mol L^{-1} sodium selenite solution was diluted with 38.75 mL of water. The pH of the solution was adjusted to approximately 3 using a 1% HCl solution, and then the solution was heated to 90 °C. Finally, 6.25 mL of a 0.04 mol L^{-1} $NaBH_4$ solution was added dropwise with constant stirring. Upon addition of the reducing agent, the solution immediately turned red, indicating the formation of a SeNPs dispersion. The dispersion was removed from the heater and maintained at the room temperature for 30 minutes under stirring. The reaction proceeded for several hours when the reacting solution was maintained at a room temperature of 25 °C.

Due to the short-term stability of the SeNP dispersion synthesized in this manner, a stabilizing agent (namely PDDA, PEI, sodium oleate, quercetin, or gelatine) was added in an appropriate quantity, depending on the type of stabilizer, to the selenite solution. All the reaction conditions, including pH, precursor concentration and reductant concentration, were applied following the same protocol as in the case of non-stabilized SeNPs. The reaction was maintained at a temperature of 90 °C for all stabilized SeNPs. The color change

from clear to orange-red occurred more slowly (after 5–20 min), depending on the stabilizer used.

In the case of reduction using ascorbic acid as a more environmentally friendly reducing agent, the procedure for non-stabilized SeNPs was similar to that of the sodium borohydride method (reduction maintained at both temperatures of 25 and 90 °C), with the exception that pH adjustments were not applied. The solution turned red gradually, and reduction was completed within 15 minutes. In order to enhance the stability of SeNP dispersions, a stabilizing agent (PDDA, PEI, sodium oleate, quercetin, or gelatine) was added to the sodium selenite solution at an appropriate concentration. This was followed by the immediate reduction using an ascorbic acid solution (0.04 mol L^{-1}). The solution was maintained at a temperature of 25 °C throughout the reduction process for the preparation of SeNPs using stabilizing agents and ascorbic acid as the reducing agent. The mixtures were stirred for a period of 15 minutes to 1 hour, depending on the stabilizer used. The color of the SeNP dispersion gradually changed from transparent to orange-red.

2.3. Characterization of SeNPs

The particle diameter and zeta potential were investigated using the Zetasizer Nano ZS (Malvern Instruments, UK). In these measurements, the synthesized SeNP dispersions were used as prepared, without any additional dilution. The morphological characterization of the SeNPs was accomplished by transmission electron microscopy (TEM) using a JEM 2010 (JEOL, Japan). For TEM characterization, the sample was diluted, applied to the mesh, and dried. The stability of the SeNP water dispersions was determined from UV-Vis absorption spectra using a UV-Vis spectrophotometer (Specord S600, Analytik Jena AG, Germany) in the range of 300–800 nm with water as a reference. The dispersions were diluted as necessary, depending on the reducing and stabilizing agents used. The structural composition of dried SeNPs was analyzed by X-ray powder diffraction (XRD) using an Aeris benchtop diffraction system (Malvern, Panalytical, Netherlands) operating in Bragg–Brentano geometry, equipped with an iron-filtered CoKα radiation source. The angular range of measurement was from 5 to 105° 2θ. The data were processed using High Score Plus software in conjunction with PDF-5 and ICSD databases. XPS measurements were carried out using the Nexsa G2 XPS system (Thermo Fisher Scientific) with a monochromatic Al-Kα source and a photon energy of 1486.7 eV. All spectra were acquired in a vacuum of 1.2×10^{-7} Pa and at a room temperature of 20 °C. The analyzed area on each sample was a spot 200 μm in diameter. For the high-resolution spectra, a pass energy of 30.00 eV and an electronvolt step of 0.1 eV were used. Charge compensation was applied for all measurements. The spectra were evaluated using the Avantage 6.5.1 (Thermo Fisher Scientific) software.

2.4. Antibacterial activity of SeNPs

The antibacterial activity was evaluated using the standard microdilution method (EUCAST[33]), based on the assessment of bacterial growth, which allows the determination of the minimal inhibitory concentration (MIC). The SeNP dispersion (1 mmol L^{-1}; 80 mg L^{-1}), or the solution of $AgNO_3$ (1 mmol L^{-1}; 108 mg L^{-1} Ag) as the reference, was diluted with cation-adjusted Mueller–Hinton broth in a geometric progression, resulting in a final tested concentration ranging from 40 to 0.625 mg L^{-1} for the SeNPs and 54 to 0.84 mg L^{-1} for $AgNO_3$. For each antibacterial assay, a fresh bacterial suspension was prepared from bacteria that had been grown on blood agar at 35 °C for 24 h. The optical density of the bacterial inoculum was adjusted to match a value of 1 based on McFarland's standards using a densitometer (Densi-La Meter, LACHEMA, Czech Republic). After appropriate dilution, this gave a starting inoculum concentration of 10^6 CFU for microbial testing using 96-well microtitration plates. The antibacterial activity was assessed according to standard testing protocols (CLSI, EUCAST) and the MIC of SeNPs and the silver salt was determined as the lowest concentration of the antibacterial agent that visibly inhibited bacterial growth after 24 h of incubation at 35 °C. For each sample, the measurement was performed three times in a single batch.

2.5. Cytotoxicity assay of SeNPs

The viability of the cells was tested using a standard MTT test, based on the conversion of the tetrazolium dye into purple formazan crystals by living cells, which determines mitochondrial activity and thus *in vitro* cytotoxic effects on the cell lines. Testing was performed on the NIH/3T3 mouse fibroblast line. The cells were cultured in Dulbecco's modified Eagle's medium at 37 °C and under a 5% CO_2 enriched atmosphere. The cells were incubated (24 h) in a 96-well plate at a density of 2×10^4 cells per well. Then, they were incubated for a further 24 h at 37 °C under a 5% CO_2 enriched atmosphere with various concentrations of SeNPs (final concentrations in DMEM: 0.625, 1.25, 2.5, 5, 10, and 20 mg L^{-1}). After the treatment, the DMEM with SeNPs was gently removed and replaced with a fresh DMEM (100 μL, containing MTT solution at a concentration of 5 mg L^{-1}). Following the incubation period (4 h), the medium containing MTT was discarded, and 100 mL of dimethylsulfoxide was added to dissolve the formazan crystals. The absorbance was then measured at a wavelength of 570 nm using an Infinite PRO M200 microplate reader (Tecan, Austria). The viability of the cells was normalized to the untreated control sample, which was set to 100% viability, and absorbance values were calculated as follows: $(A_{sample}/A_{control}) \times 100$. The half-maximal effective concentrations (EC_{50}) of the tested SeNP dispersions were extrapolated from a dose–response fit to the mean metabolic activity data using OriginPro (OriginLab Corp., Northampton, MA, USA).

3. Results and discussion

3.1. Synthesis, stabilization, and characterization of SeNPs

The synthesis of SeNP dispersions was achieved through a simple reduction method, employing either sodium boro-

hydride or ascorbic acid as the reducing agents. These agents are commonly utilized in wet chemical reduction methods. Initially, the priority was to find an optimal ratio of the precursor and the reducing agent, which would enable the formation of SeNPs with the desired particle size and outstanding stability, leading to a high level of antibacterial activity. Consequently, the impact of several stabilizing agents (PDDA, PEI, sodium oleate, quercetin and gelatine) at various concentrations (200 to 800 mg L^{-1}, respectively 0.02 to 0.08%) was also evaluated in order to produce highly stable SeNP dispersions. All stabilizers used in this study are soluble in water, with the exception of quercetin, which is known for its wide range of biological properties (antioxidant, anti-inflammatory, antimicrobial, and antiviral).[34,35] However, its solubility in water is only 60 mg L^{-1} (at 16 °C).[36] Therefore, when SeNPs were synthesized at a temperature of 25 °C, quercetin did not dissolve at the concentration of 200 mg L^{-1}. Consequently, this sample was not prepared with ascorbic acid as the reducing agent. Finally, the antimicrobial activity and cytotoxicity of the selected samples were determined.

Before the reduction process with sodium borohydride, the pH of the sodium selenite solution or its mixture with stabilizers was adjusted to approximately 3 using a 1% hydrochloric acid solution. Following the addition of sodium borohydride to the solution and the completion of the reduction process, the pH increased back to 8–9 (depending on the stabilizing agent used), due to the basicity of $NaBH_4$. Therefore, the final pH of the SeNP dispersion was alkaline. In order to accelerate the reduction process, the pH was adjusted. At lower pH values, aqueous borohydride solutions undergo hydrolysis. For the rapid reaction of borohydride and oxonium ion, the selenium species must be fully protonated.[37,38] Without pH adjustment of the reaction system, the reaction proceeded at a slower rate and was less effective.

In the second synthetic approach, in which ascorbic acid served as the reducing agent, the pH decreased to 4–5 following the addition of the reductant, and the final pH of the SeNP dispersion was acidic. Subsequently, the size, morphology, zeta potential and optical properties of the prepared SeNPs were determined using DLS, XRD, TEM and UV-Vis absorption spectroscopy. For the determination of the oxidation state of the samples, XPS was performed.

3.1.1. Morphology and size. The morphology of the synthesized SeNPs was established through transmission electron microscopy (TEM) images (Fig. 1 and S1,† respectively). The prepared SeNPs exhibited a spherical morphology, with the exception of those synthesized using sodium borohydride at a room temperature of 25 °C, which also exhibited hexagonal-

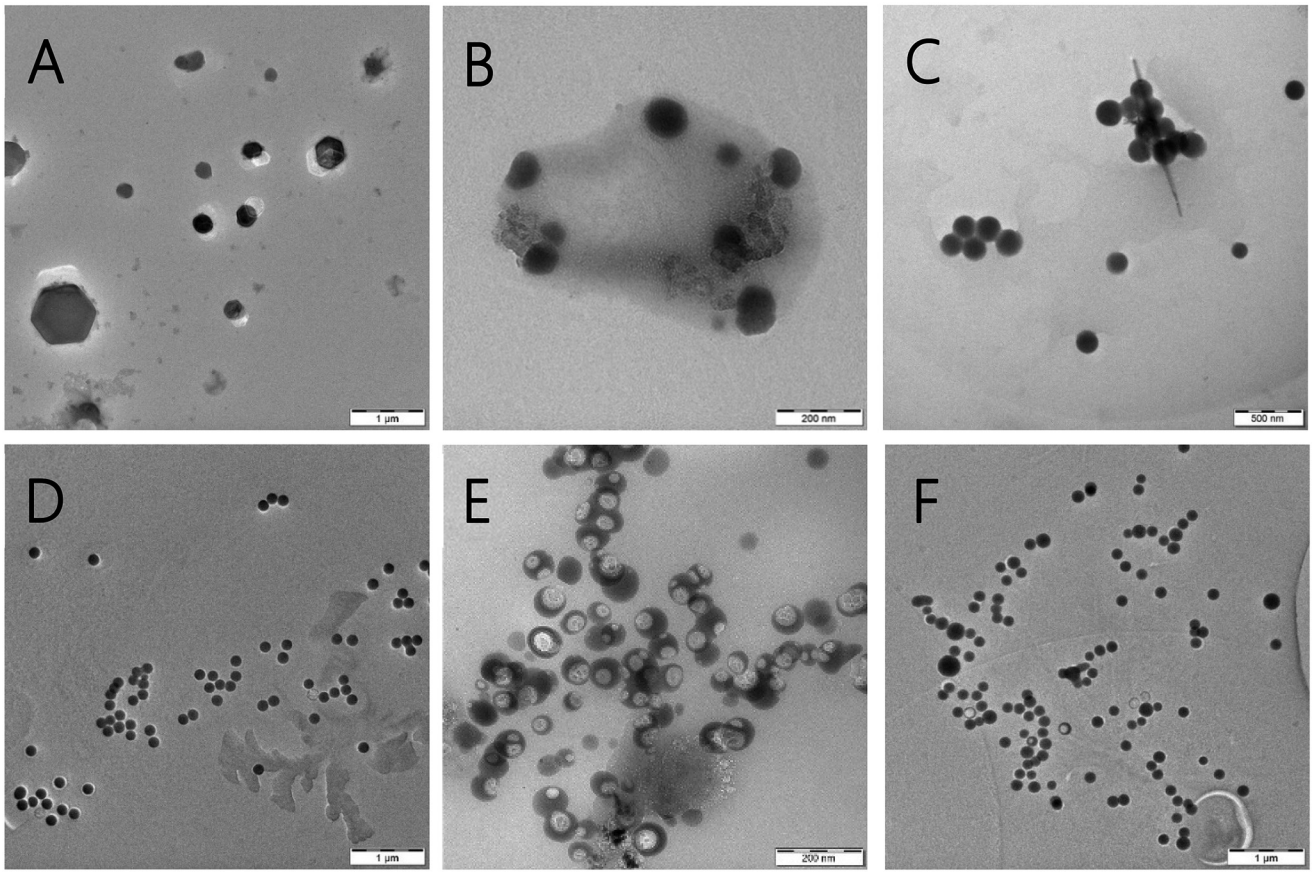

Fig. 1 TEM images of SeNP dispersions synthesized using (A) and (B) sodium borohydride at 25 °C, (C) sodium borohydride at 90 °C, (D) ascorbic acid at 25 °C, and (E and F) ascorbic acid at 90 °C.

shaped nanoparticles (see Fig. 1A). When quercetin was employed as a stabilizing agent, rod-shaped structures of quercetin were observed in the TEM images (Fig. S1E†), as well as small particles (Fig. S1F†) measuring approximately 1 nm, which are attributed to undissolved quercetin. The particle diameter of the SeNPs was determined using the dynamic light scattering (DLS) method, as detailed in Fig. 2 (and Fig. S4† with a zoom on the first 30 days). The particle size was established approximately two hours after reduction. The exception to this was the SeNPs synthesized using $NaBH_4$ at room temperature without a stabilizing agent, where the reaction lasted several hours. Consequently, the first DLS measurement of this sample was carried out 24 hours after reduction.

The average size of non-stabilized SeNPs synthesized by sodium borohydride reduction at a temperature of 25 °C was larger than that at 90 °C, measuring 280.4 nm and 122.3 nm, respectively. Both non-stabilized SeNP dispersions exhibited similar dispersity, as indicated by the PDI (polydispersity index) values of 0.382 and 0.372. Moreover, the morphology of the SeNPs prepared at a lower temperature (25 °C) differed from that of the SeNPs prepared at a higher temperature (90 °C). The PDI values for these samples were determined to be 0.141 and 0.231, respectively. TEM images revealed the presence of clusters of spherical nanoparticles with a diameter below 100 nm, as well as larger hexagonal particles with diameters in the micrometer range (see Fig. 1A and B). The particle diameters of non-stabilized SeNPs were 157.8 nm and 232.7 nm at reaction temperatures of 25 °C and 90 °C, respectively, when ascorbic acid was used. TEM images (Fig. 1E) revealed structural deformations of the nanoparticles when synthesis was conducted at a higher temperature (90 °C) using ascorbic acid. This is likely due to the rapid nature of the reaction and the inclusion of the solution into the nanoparticle sphere. The experiment was repeated, and the deformation was also observed, albeit to a lesser extent (see Fig. 1F).

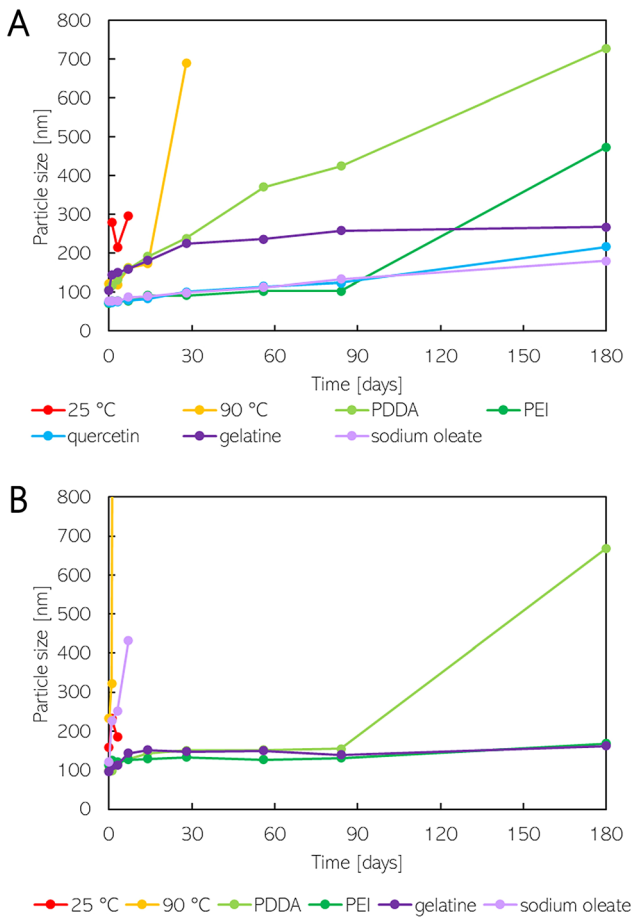

Fig. 2 The size change of SeNPs synthesized using (A) sodium borohydride and (B) ascorbic acid.

When stabilizing agents were employed, the synthesis of SeNPs proceeded at 90 °C for the borohydride method and at 25 °C for the ascorbic acid reduction, in accordance with the obtained data. Given that all stabilized SeNPs exhibited a spherical morphology (Fig. S1A–J†), it was concluded that the stabilizing agent did not influence the SeNPs' morphology. The particle diameters of the stabilized SeNPs were found to be smaller than those of the non-stabilized ones (see Fig. 2). For particles stabilized by PDDA, the PDI was 0.512 for borohydride reduction and 0.103 for ascorbic acid reduction. However, this difference may be due to the higher concentration of PDDA used for ascorbic acid reduction. The PDI for PEI-stabilized SeNPs was very similar for both reducing agents, with values of 0.087 and 0.062. The PDI values of the gelatine-stabilized SeNPs were 0.160 and 0.132, while for sodium oleate, the PDI values were 0.212 and 0.215. Consequently, the polydispersity of SeNPs increased when sodium oleate was used compared to that of non-stabilized SeNPs. In contrast, the PDI of SeNPs stabilized with gelatine remained similar to that of non-stabilized SeNPs. In the case of PEI, the PDI decreased, and the SeNP dispersions were almost monodisperse. Finally, when quercetin was used for the synthesis of SeNPs using the borohydride method, the PDI was found to be 0.121.

3.1.2. UV-Vis spectroscopy. The formation of SeNPs was observed by a visible color change from clear to red (in the case of non-stabilized SeNPs) or to orange-red (for stabilized SeNPs). The color change was attributed to the surface plasmon resonance (SPR) of SeNPs, as evidenced by previous studies.[21,27,39,40] Thanks to SPR, the SeNPs exhibit a characteristic absorption band in the wavelength range of 300 to 600 nm in the UV-Vis absorbance spectra.[6] This was confirmed for SeNPs reduced by sodium borohydride as well as by ascorbic acid (Fig. S2 and S3†). The use of stabilizing agents had a minimal effect on the absorption band, with the exception of SeNPs stabilized by quercetin, which absorbs light in the wavelength range of 350 to 400 nm (see Fig S2F†).

3.1.3. Zeta potential. Zeta potential (ZP) provides information about the electrical state and charge of nanoparticles. The charge of nanoparticles depends on their nature and the dispersion environment.[41,42] The ZPs of the prepared SeNPs are summarized in Fig. 3 (and Fig. S5† with a zoom on the first 30 days). For non-stabilized SeNPs, the charge was nega-

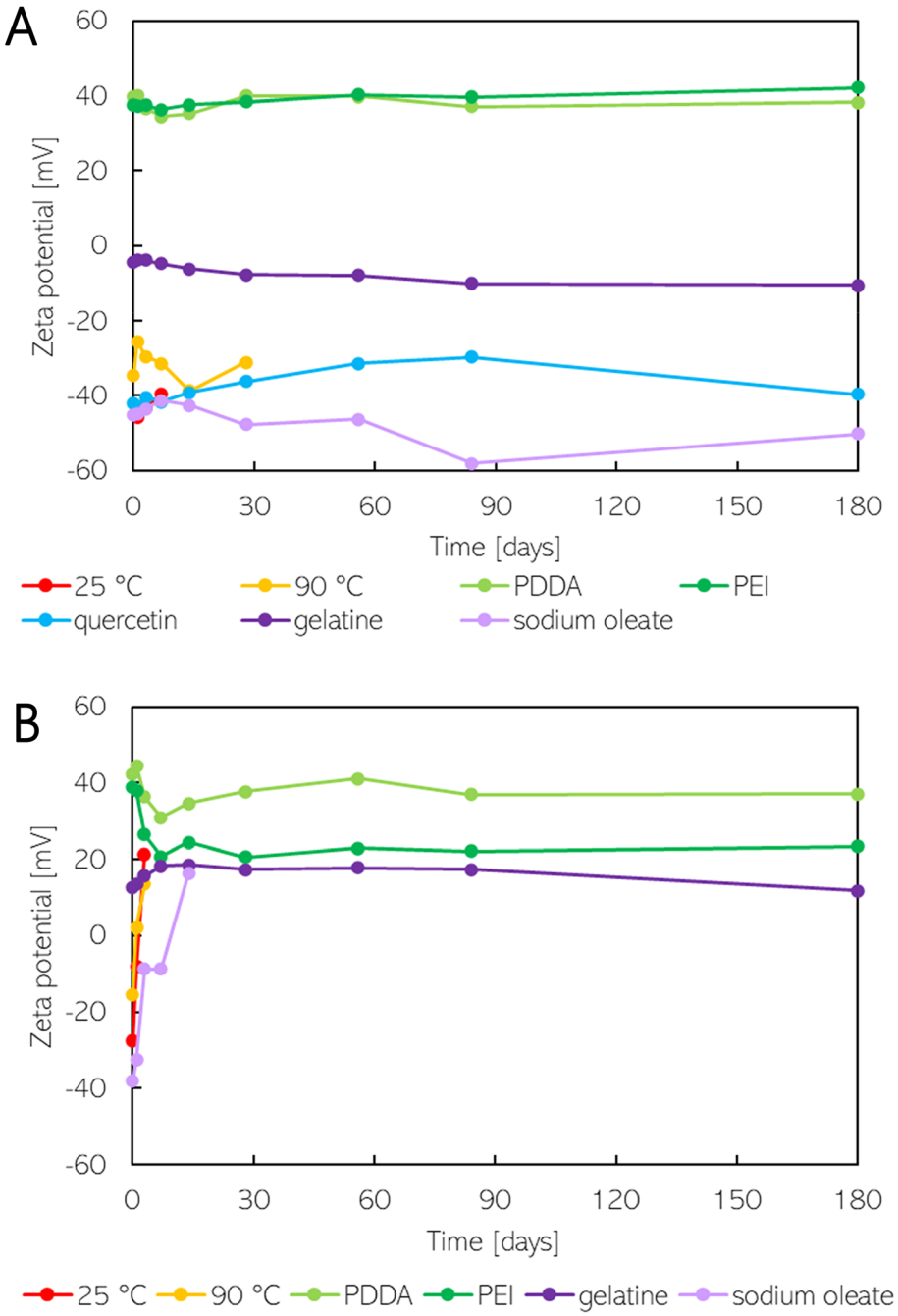

Fig. 3 The zeta potential change of SeNPs synthesized using (A) sodium borohydride and (B) ascorbic acid.

tive for both the sodium borohydride and ascorbic acid synthetic routes. Hence, the charge of the SeNPs was negative and was not influenced by the pH of the medium, given that sodium borohydride SeNP dispersions were alkaline, whereas those prepared using ascorbic acid were acidic. The addition of PDDA and PEI as stabilization agents resulted in a positive ZP value, due to the protonation of these polymeric molecules containing amine groups. On the other hand, sodium oleate maintained a negative charge on the SeNPs, regardless of the pH of the dispersion, due to the presence of $-COO^-$ groups. In contrast, the charge of SeNPs stabilized by gelatine depended on the pH of the dispersion medium, due to the amphoteric properties of gelatine. Consequently, under alkaline conditions, the SeNPs with gelatine were negatively charged (Fig. 3A) due to deprotonation, while under acidic conditions, the SeNPs were positively charged (Fig. 3B), as a result of protonated $-NH_3^+$ groups.

According to the DLVO theory, the value of ZP indicates the stability properties of nanoparticles.[41,42] Bhattacharjee (2016)[42] states that colloids with ZP values exceeding ±30 mV

are highly stable. Meanwhile, Pochapski *et al.* (2021)[41] assert that ZP values between ±30 and ±40 mV indicate moderate electrostatic stability of NPs, and values above ±40 mV correspond to electrostatically stable nanoparticles. However, the stability of colloids depends on both electrostatic and steric interactions.[41] Consequently, it is necessary to also consider steric forces when describing the stability of nanoparticles. As observed, the initial ZP does not provide a definitive indication of the stability of SeNP dispersions. Non-stabilized SeNPs (reduced by sodium borohydride at a temperature of 25° C) exhibited a high ZP value of −45.9 mV. However, as will be described in the following section, the SeNP dispersion was found to be unstable. On the other hand, despite a low ZP value of +12.6 mV, the SeNP dispersion synthesized using ascorbic acid and stabilized by gelatine was stable, likely due to the prevailing steric effects.

3.1.4. Stability. The stability of SeNPs was determined by monitoring changes in their diameter, zeta potential, and UV-Vis absorption spectra. The change in particle diameter (Fig. 2) was found to correspond to changes in the UV-vis absorption spectra (Fig. S2 and S3†). Several destabilization processes of SeNPs were observed, including aggregation over time, as indicated by the increasing size established by DLS. The visual color change from red to gray was observed in several SeNP dispersions. Sedimentation and adsorption onto the vessel's surface were also observed.

According to the literature, we first attributed this color change to a transition in the crystal structure to a trigonal (t-Se) structure of gray color.[43,44] Hence, XRD and XPS measurements were performed in order to confirm the crystal structure and oxidation state of the prepared SeNPs. The XRD patterns remained the same for both the orange- and gray-colored samples (see Fig. 4). In both samples, a hexagonal selenium lattice plane indexed to (100), (101), (110), (102), (111), and (201) was confirmed, which agrees with the standard card (PDF 04-003-6030). The lattice parameters remained the same for the stable orange-colored SeNPs sample with a = 0.437 nm and b = 0.494 nm and the destabilized gray sample with a = 0.436 nm and b = 0.495 nm. The XPS measurements revealed that selenium in gray destabilized samples exists exclusively in the Se(-II) state (Fig. 5A and C), with Se 3d5/2 and Se 3d3/2 peaks at binding energies of 54 eV and 55 eV, respectively. A mixed oxidation state of Se was observed for the stable orange-colored SeNPs. When $NaBH_4$ was used for reduction (Fig. 5B), two oxidation states of Se were observed, with 57.4% in the Se (-II) state (Se 3d5/2 at 54.553 eV and Se 3d3/2 at 55.353 eV) and 42.6% in the elemental state Se(0) (Se 3d5/2 at 55.762 eV and Se 3d3/2 at 56.562 eV). XPS of the stable SeNPs reduced by ascorbic acid (Fig. 5D) showed the most complex selenium chemistry, containing 46.5% Se(-II) (Se 3d5/2 at 54.667 eV, Se 3d3/2 at 55.435 eV), 30.7% Se(0) (Se 3d5/2 at 55.775 eV, Se 3d3/2 at 56.575 eV), and 22.8% in the Se(II) state (Se 3d5/2 at 57.565 eV, Se 3d3/2 at 58.365 eV). Therefore, the color change is not caused by a crystal structure transformation but rather by continued reduction to the final Se(-II) oxidation state and the complete disappearance of the elemental selenium state.

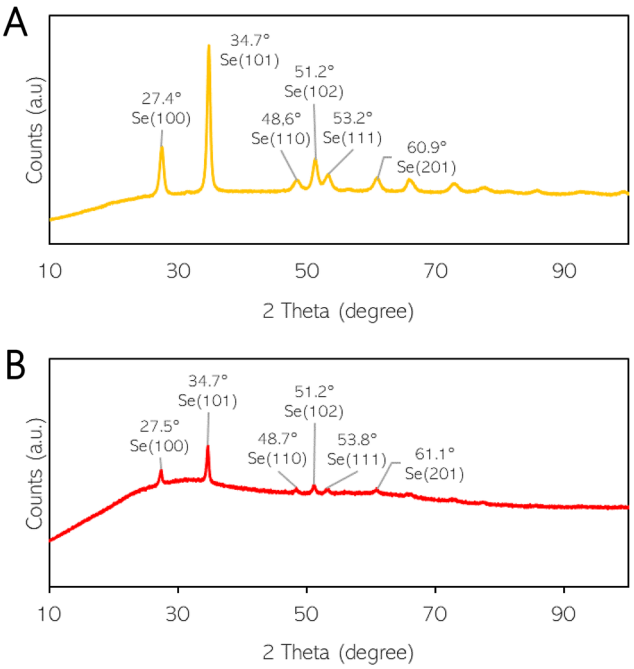

Fig. 4 The X-ray diffraction (XRD) patterns of the synthesized SeNPs reduced by ascorbic acid represented as (A) destabilized SeNPs with gray color and (B) stable SeNPs with orange color.

Non-stabilized SeNP dispersions reduced by sodium borohydride were found to be more stable when the reduction occurred at 90 °C rather than 25 °C. When the reduction occurred at room temperature, the average size of the SeNPs was larger, and hexagonal-shaped nanoparticles were observed (see Fig. 2A). The average size remained almost the same for one week; however, a color change from red to gray occurred, attributed to an oxidation state change, as discussed earlier. When SeNP dispersions were prepared at a higher temperature, the particle size changed from 122.3 to 173.4 nm within two weeks. In the fourth week, the average size of the particles reached 690.3 nm. There was no significant change in the zeta potential of the SeNPs, which had been reduced by sodium borohydride at a temperature of 25 °C. The ZP decreased from 45.9 to 39.6 mV (Fig. 3A). With an increase in the reduction temperature, the ZP of the SeNPs decreased from 34.6 to 25.5 mV within 24 hours; however, it then gradually increased up to 38.7 mV within two weeks.

In the case of the ascorbic acid reduction method, the stability of the non-stabilized SeNP dispersions was found to be the same for both synthetic temperatures. However, TEM images (Fig. 1E) showed that the particles exhibited structural disruption when a higher temperature was used for synthesis. Furthermore, the aggregation process was faster (Fig. 2B). In both cases, the change of the charge from negative to positive occurred. At a higher temperature, this change occurred within 24 hours, while at a lower temperature, it took up to 72 hours (see Fig. 3B). The SeNP dispersions synthesized using the sodium borohydride method were successfully stabilized

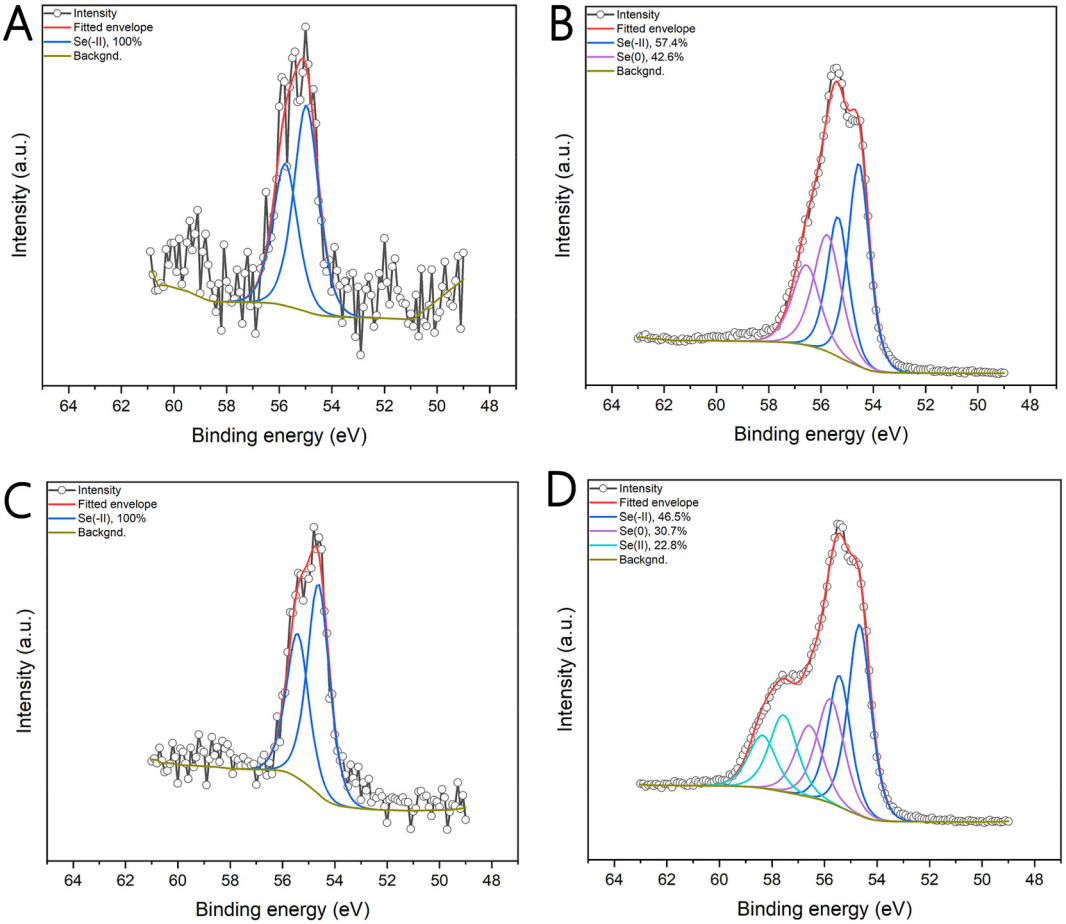

Fig. 5 The X-ray photoelectron spectra (XPS) of selenium (Se 3d) for (A) destabilized SeNPs reduced by $NaBH_4$, (B) SeNPs in a stable state reduced by $NaBH_4$, (C) gray destabilized SeNPs reduced by ascorbic acid, and (D) orange stable SeNPs reduced by ascorbic acid.

using either quercetin, gelatine, or sodium oleate. The particle sizes after reduction were 73.9, 105.6, and 77.0 nm, respectively, and gradually increased over time. However, the size change was less than three times the original size (see Fig. 2A). The ZP values for PEI- or sodium oleate-stabilized SeNPs remained constant for the first two weeks, after which a slight increase was observed (Fig. 3A). In contrast, for the quercetin-stabilized SeNPs, the ZP remained constant for the first two weeks, before decreasing from the original value of 42.0 to 29.7 mV after eight weeks. When the ZP of this sample was remeasured six months later, the value increased back to 39.7 mV. It can be concluded that quercetin, gelatine, and sodium oleate are the optimal choice for stabilizing SeNP dispersions synthesized using sodium borohydride, among the tested stabilization agents. Neither PDDA nor PEI was found to be effective in stabilizing SeNPs to the same extent. It can be stated that stabilizing agents with negatively charged groups were effective in stabilizing the synthesized SeNPs.

On the other hand, the stability of the SeNPs synthesized using ascorbic acid can be achieved by employing a stabilizing agent with protonated $-NH_3^+$ groups rather than negatively charged $-COO^-$ groups. The size change of SeNPs stabilized using PEI and gelatine was less than twice the original size (Fig. 2B). Moreover, the size of the SeNPs increased from 113.3 to 168.5 nm over a six-month period, when PEI was used for stabilization. The zeta potential of PDDA- and PEI-stabilized SeNPs decreased from the original value of 42.4 to 31.0 mV, respectively, from 38.8 to 20.7 mV in the first week (see Fig. 3B). Subsequently, the ZP slightly increased but remained at a nearly constant value. In the case of gelatine-stabilized SeNPs, the ZP initially increased from its original value of 12.6 to 18.3 mV within the first week and then remained the same for the next eight weeks. After six months, the ZP decreased below the original value. The stability of the SeNPs prepared using ascorbic acid as a reductant and sodium oleate as a stabilizer was found to be poor. Within the first week, the particles underwent gradual aggregation. Furthermore, the charge of the SeNPs transitioned from negative to positive over two weeks.

In conclusion, the most stable SeNP dispersions were obtained when gelatine was used as a stabilizing agent for both synthetic approaches (reduction with sodium borohydride and ascorbic acid). Moreover, the stability of SeNP dispersions could be prolonged using quercetin or sodium oleate

in sodium borohydride reduction. In the case of the ascorbic acid synthetic method, the use of PEI as a stabilizing agent resulted in good stability. Based on the results, we conclude that the pH and zeta potential (ZP) charge of SeNP dispersions influence the effectiveness of the stabilizing agent (depending on the selected reducing agent) the most. SeNP dispersions prepared using $NaBH_4$ are alkaline, and the ZP charge is negative. Hence, the stabilizing agent with a $-COO^-$ functional group is optimal. On the other hand, SeNP dispersions synthesized using ascorbic acid are acidic, and the ZP is also negative. Changing the ZP from negative to positive using a stabilizing agent with a $-NH_3^+$ functional group can ensure SeNP dispersion stability.

3.2. Antibacterial activity

The antibacterial activity of SeNPs was determined as a minimal inhibitory concentration (MIC) of the tested nanoparticles, which visually inhibits bacterial growth. This was tested on both Gram-negative and Gram-positive bacterial strains (summarized in Tables 1 and 2). Non-stabilized SeNPs prepared by sodium borohydride reduction were active against *E. faecalis* and *S. aureus* with MIC 20 and 40 mg L^{-1}, respectively. Non-stabilized nanoparticles prepared using the ascorbic acid approach demonstrate no activity against any of the tested Gram-positive strains, with the exception of methicillin-resistant *S. aureus* (MRSA) up to the concentration of 40 mg L^{-1}. The antibacterial activity of SeNPs synthesized using ascorbic acid was just slightly improved in the case of stabilization with gelatine, with a significant enhancement of antibacterial activity against MRSA, with a MIC of 0.3 mg L^{-1}. This concentration is considerably lower than that of ionic silver (6.8 mg L^{-1}), which is considered to have strong antibacterial properties. In the case of ascorbic acid as a reductant and PEI as a stabilizer, stabilization improved the antibacterial activity against all of the tested Gram-positive strains, with better results against staphylococcal strains (Table 2). The antibacterial activity of quercetin-stabilized SeNPs was not measured due to its low solubility (60 mg L^{-1} at 16 °C in water[36]) at the room temperature used for synthesis. The nanoparticles with the most promising observed antibacterial properties were stabilized by PDDA, with MIC values ranging from 0.3 to 2.5 mg L^{-1} for Gram-positive strains. Moreover, they were also active against Gram-negative strains, including *E. coli* (20 mg L^{-1}) and *P. aeruginosa* (2.5 mg L^{-1}). This represents a significantly greater activity against Gram-negative bacteria than previously reported for SeNPs prepared by chemical reduction. Huang *et al.* (2016) synthesized SeNPs using $NaBH_4$ (and acetic acid for pH adjustment) with MIC against *E. coli*, *P. aeruginosa*, and *S. aureus* at concentrations of 32, 24, and 8 mg l^{-1}, respectively.[5] In ascorbic acid reduction, SeNPs stabilized by PVA showed no activity against *S. aureus*, and against *E. coli* and *P. aeruginosa*, the MIC was high at 11 and 12.5 ppm.[23] However, in another study with the same reactants, the MIC of SeNPs was 250 mg l^{-1} for *E. coli* and *P. aeruginosa* and 125 mg l^{-1} for *S. aureus.*[21] Lower antimicrobial activity was detected by Filipović *et al.* (2021) for SeNPs synthesized using ascorbic acid and BSA (bovine serum albumin) as a stabilization agent, with the MIC of 100 ppm against *S. aureus* and 400 ppm against *E. coli* and *P. aeruginosa*.[45]

In order to exclude the effect of the stabilizing agent itself and to explain its effect on the antibacterial activity of the nanoparticles, the antibacterial activity of each stabilizer was

Table 1 Antibacterial activity of SeNPs synthesized using sodium borohydride and stabilized by various stabilizing agents (PDDA, sodium oleate, quercetin, and gelatine) expressed as the minimum inhibitory concentration (MIC)

	MIC [mg l^{-1}]				
Bacterial strain	SeNPs	SeNPs 0.02% PDDA	SeNPs 0.02% sodium oleate	SeNPs 0.02% quercetin	SeNPs 0.02% gelatine
E. coli 3954	>40.0	20.0	>40.0	>40.0	>40.0
P. aeruginosa 3955	>40.0	5.0	>40.0	>40.0	>40.0
VRE 419	>40.0	20.0	>40.0	>40.0	40.0
E. faecalis 4224	20.0	10.0	5.0	>40.0	40.0
S. aureus 4223	40.0	5.0	5.0	40.0	40.0
MRSA 4591	>40.0	5.0	1.3	5.0	40.0

Table 2 Antibacterial activity of SeNPs synthesized by ascorbic acid reduction and stabilized by various stabilizing agents (PDDA, PEI, quercetin, and gelatine) expressed as the minimum inhibitory concentration (MIC)

	MIC [mg l^{-1}]				
Bacterial strain	Ag^+ ions	SeNPs	SeNPs 0.04% PDDA	SeNPs 0.08% PEI	SeNPs 0.02% gelatine
E. coli 3954	3.4	>40.0	20.0	>40.0	>40.0
P. aeruginosa 3955	1.7	>40.0	2.5	>40.0	>40.0
VRE 419	6.8	>40.0	1.3	20.0	>40.0
E. faecalis 4224	6.8	>40.0	2.5	40.0	>40.0
S. aureus 4223	6.8	>40.0	0.3	10.0	40.0
MRSA 4591	13.5	40.0	0.3	5.0	0.3

Table 3 Antibacterial activity of stabilizing agent solutions expressed as the minimum inhibitory concentration (MIC) of the used stabilizer

	MIC [mg l^{-1}]					
Bacterial strain	Sodium selenite	0.02% PDDA solution	0.02% sodium oleate solution	0.08% PEI solution	0.02% quercetin solution	0.02% gelatine solution
E. coli 3954	>40.0	50.0	>200.0	>800.0	>200.0	>200.0
P. aeruginosa 3955	>40.0	25.0	>200.0	100.0	>200.0	>200.0
VRE 419	40.0	12.5	>200.0	200.0	>200.0	>200.0
E. faecalis 4224	>40.0	12.5	>200.0	200.0	>200.0	>200.0
S. aureus 4223	40.0	3.1	>200.0	100.0	>200.0	>200.0
MRSA 4591	20.0	1.6	25.0	25.0	>200.0	>200.0

Table 4 Antibacterial activity of stabilizing agents (PDDA, sodium oleate, and PEI) in the SeNP dispersion (SeNPs reduced by either sodium borohydride or ascorbic acid) expressed as the minimum inhibitory concentration (MIC)

	MIC [mg l^{-1}]			
Bacterial strain	SeNPs 0.02% PDDA (borohydride)	SeNPs 0.02% sodium oleate (borohydride)	SeNPs 0.04% PDDA (ascorbic acid)	SeNPs 0.08% PEI (ascorbic acid)
E. coli 3954	50	>100	100	>400
P. aeruginosa 3955	12.5	>100	12.5	>400
VRE 419	50	>100	6.25	200
E. faecalis 4224	25	12.5	12.5	400
S. aureus 4223	12.5	12.5	1.5625	100
MRSA 4591	12.5	3.125	1.5625	50

tested (Table 3). The solutions of quercetin and gelatine did not demonstrate any antibacterial activity at the used concentrations. The sodium oleate solution demonstrated some antibacterial activity against MRSA, although at a concentration that was much higher than that used in the SeNP dispersions. On the other hand, PDDA and PEI exhibited some antibacterial properties (Tables 3 and 4). In the case of nanoparticles prepared by ascorbic acid reduction and stabilized with PDDA, the stabilizer itself demonstrated lower antibacterial properties than when tested in combination with SeNPs. Conversely, when PDDA was used for stabilization during reduction with sodium borohydride, the concentration of PDDA in the SeNPs solution was higher than its respective MIC. The results for PEI are inconclusive. The antibacterial activity of the nanoparticles stabilized with PEI was approximately equal to the MIC of PEI alone, indicating that the antibacterial properties of the nanoparticles may be solely attributable to the stabilizing agent.

SeNPs prepared by reduction with sodium borohydride and stabilized with sodium oleate exhibited slightly higher activity than those stabilized with PEI. However, this was observed only against Gram-positive strains with MIC values of 5 mg L^{-1} for both *E. faecalis* and *S. aureus*, and even lower (1.3 mg L^{-1}) for MRSA. Similarly, borohydride reduction with the PDDA stabilizer resulted in the preparation of nanoparticles that exhibited antibacterial activity against all strains tested, including Gram-negative strains (Tables 1 and 2). However, as previously discussed, this could be attributed to the stabilizing agent itself. SeNPs stabilized with gelatine exhibited antibacterial activity against Gram-positive strains with an MIC of 40 mg L^{-1}. While quercetin-stabilized nanoparticles exhibited activity only against *S. aureus* and MRSA with MIC values of 40 and 5 mg L^{-1}, respectively.

All the tested strains were also combined with silver ions, which have been demonstrate to have an antibacterial effect on both Gram-positive and Gram-negative bacterial strains (see Table 2). The SeNPs prepared by reduction using ascorbic acid and stabilized by PDDA have been found to have a lower minimal inhibitory concentration than silver ions in all of the tested bacteria except *E. coli* and *P. aeruginosa* 3955. This suggests that the nanoparticles may be a promising agent in antibacterial therapy. The surface charge of the nanoparticles plays an essential role in determining their interactions with bacteria.[6,46] Both types of bacteria have negatively charged cell walls at neutral pH: in Gram-positive bacteria due to teichoic acids, while in Gram-negative bacteria due to lipopolysaccharides.[47–49] According to the DLVO theory, when the charges of nanoparticles and bacteria are identical, it is anticipated that strong repulsive electrostatic forces will be generated between these two elements.[6,46] Consequently, negatively charged SeNPs exhibit lower adsorption to the surface of the bacterial cell wall. Therefore, it was anticipated that SeNPs with a positively charged surface would exhibit rather higher antibacterial activity. This was partly confirmed in our study, where the nanoparticles with the highest positive zeta-potential exhibited the highest antibacterial activity (SeNPs stabilized by PDDA and PEI). However, other factors, such as nanoparticle stabilization, could affect the overall antibacterial

activity. It is therefore not possible to draw a direct correlation between the surface charge of bacteria and nanoparticles and the inhibition of the bacteria. In contrast, it has been observed that chemically prepared SeNPs are more effective against Gram-positive bacteria than against Gram-negative ones, which is consistent with the previously published results.[5,6,21] This is likely due to the fact that Gram-negative bacteria have a more complex cell wall, which makes it more challenging for SeNPs to penetrate and reach the inner membrane.[48,49]

It has not been demonstrated that the reducing agent has a direct effect on the antibacterial properties since the size of the prepared SeNPs was similar. The antibacterial activity of PDDA- and PEI-stabilized SeNPs was found to be slightly impacted by the stabilizer itself. In the case of PDDA as a stabilizer and ascorbic acid as a reductant, the MIC of PDDA in the SeNP dispersion stabilized by this agent was higher than that of the PDDA solution alone. Therefore, the antibacterial effect can be attributed to the SeNPs. On the other hand, the MIC of PEI in the SeNP dispersion was comparable to that of the stabilizer alone, indicating that the antibacterial properties can be attributed to the stabilizer. Finally, as shown in Table 4, the MIC of the stabilizer increased in the SeNP dispersion prepared using the borohydride reduction method and stabilized with PDDA. This suggests that the stabilizer itself loses its antibacterial properties when it is not present in the medium in its free form, but rather as a coating onto the nanoparticle surface.

3.3. Cytotoxicity assay

The *in vitro* cytotoxicity of SeNPs was assessed using the MTT assay against the normal cell line NIH/3T3 (mouse embryonic fibroblasts). The concentrations of diluted SeNPs used were in the range of 0.625 to 20 mg L^{-1}. Cytotoxicity was evaluated by determining the EC_{50} values. The half-maximal effective concentration (EC_{50}) is defined as the amount of SeNPs required to inhibit a given process by 50%, in this case, the viability of the tested cells.

The results demonstrated that the non-stabilized SeNP dispersion prepared using $NaBH_4$ was not cytotoxic even at the highest concentration tested (20 mg L^{-1}), with an EC_{50} value exceeding 100 mg L^{-1} (see Fig. 6). Cytotoxicity of SeNPs increased when stabilizing agents were employed (with the EC_{50} ranging from 30–33 mg L^{-1}). For comparison, the EC_{50} of sodium selenite against the NIH/3T3 cell line was 7.6 mg L^{-1}. Therefore, the lower cytotoxicity of SeNPs (sodium borohydride reduction) compared to Na_2SeO_3 was confirmed. Interestingly, SeNPs prepared using ascorbic acid (a mild environmentally friendly agent) were more cytotoxic than those synthesized with a strong reductant, sodium borohydride. As illustrated in Fig. 6, when ascorbic acid was employed as a reducing agent, EC_{50} values were observed to be within the range of 2 to 9 mg L^{-1} for both non-stabilized and stabilized SeNPs. For ascorbic acid, at the same concentration as the final concentration in the prepared SeNP dispersions, accounting for 0.005 mol L^{-1}, an EC_{50} value of 35.5 mg L^{-1} was established. It has been reported that for SeNPs prepared using ascorbic acid, the NIH/3T3 cell viability was approximately 80% at a concentration of 10 mg L^{-1}.[50] However, in the study conducted by Shin *et al.* (2022),[50] the prepared SeNP dispersion was centrifuged and washed, and the SeNPs were free of ascorbic acid prior to cytotoxicity testing.

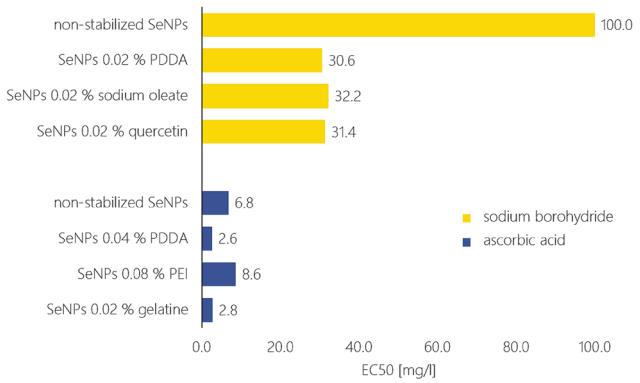

Fig. 6 Established EC_{50} values for SeNP dispersions synthesized using sodium borohydride (yellow) and ascorbic acid (blue) and stabilized by varying stabilizing agents.

Fig. 7 illustrates that cell viability decreased to 76.4% compared to the control at the lowest concentration of SeNPs reduced by $NaHB_4$. Thereafter, cell viability showed a slight decrease with increasing concentration of SeNPs. In contrast, the viability of cells at the lowest concentration of SeNPs synthesized using ascorbic acid was 6.1%. The EC_{50} of the ascorbic acid solution (at the same concentration as used in the SeNP dispersions) was found to be 22.7 mg L^{-1}. Therefore, the high cytotoxicity of the SeNPs prepared using ascorbic acid may be due to the additive toxic effect of the SeNPs and ascorbic acid. Although ascorbic acid is an antioxidant, it can also act as a pro-oxidant when high doses are used. The cytotoxicity of ascorbic acid is mediated by its conversion of free radicals into hydrogen peroxide, which can damage the cell membrane and DNA.[51,52] The combination of SeNPs and ascorbic acid and their combined cytotoxic effect could be applicable for cancer treatment, for example.

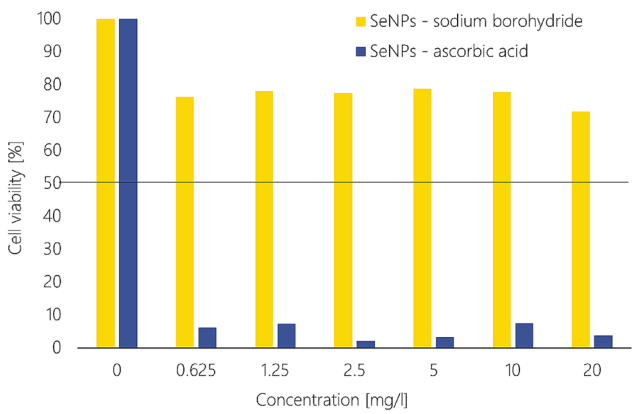

Fig. 7 Comparison of cell viability for the SeNPs synthesized using sodium borohydride (yellow) and ascorbic acid (blue).

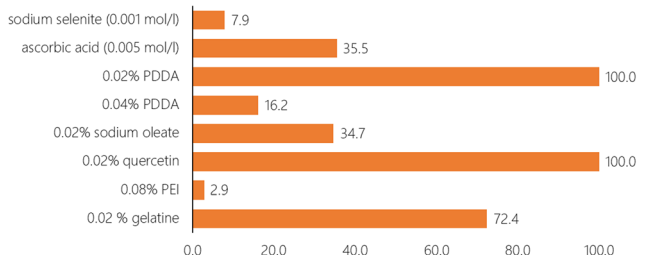

Fig. 8 Established EC_{50} values for solutions of used stabilizing agents.

Regarding the cytotoxicity of stabilizing agent solutions, PDDA and quercetin showed no cytotoxic effect at all (see Fig. 8), with EC_{50} values higher than 100 mg L^{-1}. Gelatine and sodium oleate exhibited low cytotoxicity, with EC_{50} values of 72.4 and 34.7 mg L^{-1}, respectively. In contrast, the PEI solution exhibited a markedly higher cytotoxic effect, with an EC_{50} value of 2.9 mg L^{-1}, compared to the PEI-stabilized SeNPs, which exhibited an EC_{50} value of 8.6 mg L^{-1}. The other stabilizing agent solutions were less cytotoxic compared to the stabilized SeNPs solutions (Fig. 8).

4. Conclusion

In this study, SeNPs were successfully synthesized using two different reducing agents – sodium borohydride as a strong agent and ascorbic acid as a more environmentally friendly reductant. The resulting SeNPs were spherical with a particle size of approximately 100 nm (established by DLS measurements). Non-stabilized SeNPs were only stable for up to two weeks when synthesized using the sodium borohydride reduction approach at a temperature of 90 °C. The stability can be prologed to at least 6 months when using gelatine as a stabilizing agent for both synthetic approaches. The stability of SeNP dispersions prepared using the sodium borohydride method could be prolonged using stabilizing agents with negatively charged functional groups ($-COO^-$ or $-O^-$) such as quercetin and sodium oleate. For ascorbic acid reduction, stability could be achieved using positively charged stabilizers such as PEI with $-NH_3^+$ functional groups. Several destabilizing processes were observed. Besides aggregation and sedimentation, a color change from red to gray occurred. This change occurred due to the continued reduction in prepared SeNP water dispersion to the final Se(-II) oxidation state. Most of the SeNP dispersions exhibited antibacterial activity only against Gram-positive bacteria. Outstanding antibacterial activity was detected for SeNPs, synthesized using ascorbic acid and stabilized with PDDA or gelatine, against the MRSA strain with an MIC of 0.3 mg L^{-1}. SeNPs stabilized with PDDA were also active against the Gram-negative bacteria *E. coli* (MIC 20 mg) and *P. aeruginosa* (2.5 mg L^{-1}). Interestingly, SeNPs synthesized using ascorbic acid were more cytotoxic than those prepared using sodium borohydride, with EC_{50} values higher than 100 mg L^{-1} for non-stabilized SeNPs prepared by $NaBH_4$ reduction and 6.8 mg L^{-1} for non-stabilized SeNPs prepared using ascorbic acid, respectively. SeNPs demonstrated antibacterial activity similar to ionic silver. However, silver is a heavy metal element, while selenium is a metalloid. Besides, selenium is an essential trace element. These results suggest potential applications of SeNPs in the field of medical treatment or food processing, since the stability of prepared dispersions must be known for storage. However, further investigation into the resistance of SeNPs is necessary, along with a more comprehensive understanding of their antibacterial activity mechanism.

Author contributions

Aneta Bužková: conceptualization, methodology, investigation, and writing – original draft; Lucie Hochvaldová: investigation and writing – original draft; Renata Večeřová: investigation, methodology, and writing – review & editing; Tomáš Malina: investigation and writing – review & editing; Martin Petr: investigation and writing – original draft; Josef Kašlík: investigation; Libor Kvítek: resources and writing – review & editing; Milan Kolář: resources and writing – review & editing; Aleš Panáček: resources, supervision, and writing – original draft; and Robert Prucek: conceptualization, methodology, resources, supervision, and writing – review & editing.

Data availability

Data will be available on request.

Conflicts of interest

The authors declare no conflict of interest.

Acknowledgements

The authors are thankful to Alexandra Rancová and Jana Stránská for TEM images and also to Šárka Hradilová for the partial cytotoxicity measurement. The authors gratefully acknowledge financial support from the Ministry of Health of the Czech Republic (project NU20-05-00165), and the Internal Student Grant Agency of the Palacký University in Olomouc, Czech Republic (IGA_ PrF_2024_021 and IGA_PrF_2024_020). The authors acknowledge the Research Infrastructure NanoEnviCz, supported by the Ministry of Education, Youth and Sports of the Czech Republic under Project No. LM2023066, and the National Institute of Virology and Bacteriology project (Programme EXCELES, ID Project No. LX22NPO5103) – funded by the European Union – Next Generation EU.

References

1 D. P. Biswas, N. M. O'Brien-Simpson, E. C. Reynolds, A. J. O'Connor and P. A. Tran, *J. Colloid Interface Sci.*, 2018, **515**, 78–91.

2 L. D. Geoffrion, T. Hesabizadeh, D. Medina-Cruz, M. Kusper, P. Taylor, A. Vernet-Crua, J. Chen, A. Ajo, T. J. Webster and G. Guisbiers, *ACS Omega*, 2020, **5**, 2660–2669.
3 World Health Organization, *Global action plan on antimicrobial resistance*, Geneva, 2015.
4 L. Hochvaldová, R. Večeřová, M. Kolář, R. Prucek, L. Kvítek, L. Lapčík and A. Panáček, *Nanotechnol. Rev.*, 2022, **11**, 1115–1142.
5 X. Huang, X. Chen, Q. Chen, Q. Yu, D. Sun and J. Liu, *Acta Biomater.*, 2016, **30**, 397–407.
6 P. A. Tran, N. O'Brien-Simpson, E. C. Reynolds, N. Pantarat, D. P. Biswas and A. J. O'Connor, *Nanotechnology*, 2016, **27**, 10.
7 S. Hayat, *Front. Biosci.*, 2018, **10**, 827.
8 M. Natan and E. Banin, *FEMS Microbiol. Rev.*, 2017, **41**, 302–322.
9 A. Panáček, L. Kvítek, M. Smékalová, R. Večeřová, M. Kolář, M. Röderová, F. Dyčka, M. Šebela, R. Prucek, O. Tomanec and R. Zbořil, *Nat. Nanotechnol.*, 2018, **13**, 65–71.
10 M. A. Argudín, A. Hoefer and P. Butaye, *Res. Vet. Sci.*, 2019, **122**, 132–147.
11 N. Hadrup, A. K. Sharma and K. Loeschner, *Regul. Toxicol. Pharmacol.*, 2018, **98**, 257–267.
12 B. Hosnedlova, M. Kepinska, S. Skalickova, C. Fernandez, B. Ruttkay-Nedecky, Q. Peng, M. Baron, M. Melcova, R. Opatrilova, J. Zidkova, G. Bjørklund, J. Sochor and R. Kizek, *Int. J. Nanomed.*, 2018, **13**, 2107–2128.
13 K. Brown and J. Arthur, *Public Health Nutr.*, 2001, **4**, 593–599.
14 H. R. El-Ramady, É. Domokos-Szabolcsy, N. A. Abdalla, T. A. Alshaal, T. A. Shalaby, A. Sztrik, J. Prokisch and M. Fári, *Environ. Chem. Lett.*, 2014, **12**, 495–510.
15 S. Skalickova, V. Milosavljevic, K. Cihalova, P. Horky, L. Richtera and V. Adam, *Nutrition*, 2017, **33**, 83–90.
16 K. S. Prasad, H. Patel, T. Patel, K. Patel and K. Selvaraj, *Colloids Surf., B*, 2013, **103**, 261–266.
17 B. Gates, B. Mayers, B. Cattle and Y. Xia, *Adv. Funct. Mater.*, 2002, **12**, 219–227.
18 Q. Wang, A. Mejía-Jaramillo, J. J. Pavon and T. J. Webster, *J. Biomed. Mater. Res., Part B*, 2016, **104**, 1352–1358.
19 P. A. Tran and T. J. Webster, *Nanotechnology*, 2013, **24**, 7.
20 V. Bartůněk, J. Junková, J. Šuman, K. Kolářová, S. Rimpelová, P. Ulbrich and Z. Sofer, *Mater. Lett.*, 2015, **152**, 207–209.
21 S. Boroumand, M. Safari, E. Shaabani, M. Shirzad and R. Faridi-Majidi, *Mater. Res. Express*, 2019, **6**, 9.
22 Z. Wang, J. Jing, Y. Ren, Y. Guo, N. Tao, Q. Zhou, H. Zhang, Y. Ma and Y. Wang, *Mater. Lett.*, 2019, **234**, 212–215.
23 B. A. Al Jahdaly, N. S. Al-Radadi, G. M. G. Eldin, A. Almahri, M. K. Ahmed, K. Shoueir and I. Janowska, *J. Mater. Res. Technol.*, 2021, **11**, 85–97.
24 D. Medina Cruz, G. Mi and T. J. Webster, *J. Biomed. Mater. Res., Part A*, 2018, **106**, 1400–1412.
25 S. Pandey, N. Awasthee, A. Shekher, L. C. Rai, S. C. Gupta and S. K. Dubey, *Bioprocess Biosyst. Eng.*, 2021, **44**, 2679–2696.
26 B. Fardsadegh and H. Jafarizadeh-Malmiri, *Green Process. Synth.*, 2019, **8**, 399–407.
27 S. Menon, K. S. Shrudhi Devi and V. K. Shanmugam, *Colloid Interface Sci. Commun.*, 2019, **29**, 8.
28 Y. Ma, L. Qi, W. Shen and J. Ma, *Langmuir*, 2005, **21**, 6161–6164.
29 E. Filippo, D. Manno and A. Serra, *Chem. Phys. Lett.*, 2011, **510**, 87–92.
30 K. Mondal and S. K. Srivastava, *Mater. Chem. Phys.*, 2010, **124**, 535–540.
31 K. Badgar and J. Prokisch, *Molecules*, 2021, **26**, 6457.
32 S. Chhabria and K. Desai, in *Encyclopedia of Nanoscience and Nanotechnology*, 2016, pp. 32.
33 EUCAST, *The European Committee on Antimicrobial Susceptibility Testing*, **https://www.eucast.org/**, (accessed 31 August 2022).
34 A. K. Mittal, S. Kumar and U. C. Banerjee, *J. Colloid Interface Sci.*, 2014, **431**, 194–199.
35 A. Di Petrillo, G. Orrù, A. Fais and M. C. Fantini, *Phytother. Res.*, 2021, 1–13.
36 National Center for Biotechnology Information, P. Database, Quercetin CID=5280343, **https://pubchem.ncbi.nlm.nih.gov/compound/5280343**, (accessed 31 August 2022).
37 A. Ramesh Kumar and P. Riyazuddin, *Int. J. Environ. Anal. Chem.*, 2007, **87**, 469–500.
38 S. Amendola, *Talanta*, 1999, **49**, 267–270.
39 N. Srivastava and M. Mukhopadhyay, *Bioprocess Biosyst. Eng.*, 2015, **38**, 1723–1730.
40 K. Anu, G. Singaravelu, K. Murugan and G. Benelli, *J. Cluster Sci.*, 2017, **28**, 551–563.
41 D. J. Pochapski, C. Carvalho dos Santos, G. W. Leite, S. H. Pulcinelli and C. V. Santilli, *Langmuir*, 2021, **37**, 13379–13389.
42 S. Bhattacharjee, *J. Controlled Release*, 2016, **235**, 337–351.
43 P. Cherin and P. Unger, *Inorg. Chem.*, 1967, **6**, 1589–1591.
44 T. M. Sakr, M. Korany and K. V. Katti, *J. Drug Delivery Sci. Technol.*, 2018, **46**, 223–233.
45 N. Filipović, D. Ušjak, M. T. Milenković, K. Zheng, L. Liverani, A. R. Boccaccini and M. M. Stevanović, *Front. Bioeng. Biotechnol.*, 2021, **8**, 624621.
46 A. S. Joshi, P. Singh and I. Mijakovic, *Int. J. Mol. Sci.*, 2020, **21**, 7658.
47 B. Gottenbos, *J. Antimicrob. Chemother.*, 2001, **48**, 7–13.
48 M. J. Hajipour, K. M. Fromm, A. A. Ashkarran, D. Jimenez de Aberasturi, I. R. de Larramendi, T. Rojo, V. Serpooshan, W. J. Parak and M. Mahmoudi, *Trends Biotechnol.*, 2012, **30**, 499–511.
49 Y. N. Slavin, J. Asnis, U. O. Häfeli and H. Bach, *J. Nanobiotechnol.*, 2017, **15**, 20.
50 S. Shin, K. Saravanakumar, A. V. A. Mariadoss, X. Hu, A. Sathiyaseelan and M.-H. Wang, *J. Nanostruct. Chem.*, 2022, **12**, 23–32.
51 L. Tronci, G. Serreli, C. Piras, D. V. Frau, T. Dettori, M. Deiana, F. Murgia, M. L. Santoru, M. Spada, V. P. Leoni, J. L. Griffin, R. Vanni, L. Atzori and P. Caria, *Antioxidants*, 2021, **10**, 809.
52 J. J. Casciari, N. H. Riordan, T. L. Schmidt, X. L. Meng, J. A. Jackson and H. D. Riordan, *Br. J. Cancer*, 2001, **84**, 1544–1550.